Polymer 290 (2024) 126522

Contents lists available at ScienceDirect

Polymer

journal homepage: www.elsevier.com/locate/polymer

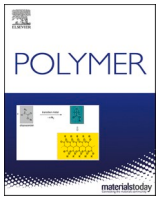

Effect of the chain length of geraniol esters on the plasticization efficiency with poly(lactide)

J. Gomez-Caturla [a,*], J. Ivorra-Martinez [a], R. Tejada-Oliveros [a], V. Moreno [a], D. Garcia-Garcia [a], R. Balart [a]

[a] Institute of Materials Technology (ITM), Universitat Politècnica de València (UPV), Plaza Ferrándiz y Carbonell 1, 03801, Alcoy, Alicante, Spain

ARTICLE INFO

Keywords:
Poly(lactic acid)
Plasticizer
Geraniol ester
Ductility
Mechanical properties

ABSTRACT

This work reports on the development of environmentally friendly PLA formulations utilizing different esters derived from geraniol as plasticizers. Geranyl formate, acetate, propionate, butyrate, isovalerate and caproate at 10 wt% were combined with PLA in formulations that were produced through extrusion and injection moulding processes. Theoretical solubility parameter studies predicted good miscibility between PLA and all the plasticizers. This was confirmed by tensile test, which showed elongation at break values between 200 and 300 %, totally in contrast with the 8 % value of neat PLA. Geranyl acetate and geranyl formate exhibited the highest elongation at break behavior. These values of elongation at break were supported by FESEM images, which showed clear signs of plasticization. The plasticization effect was further corroborated by DSC and DMTA analysis, where a clear decrease in the glass transition temperature was observed from a typical value of 60 °C for neat PLA down to 40–50 °C for the plasticized blends. This was related to an enhanced chain mobility of the amorphous regions of PLA. Moreover, the plasticizers slightly increased the water absorption capabilities of PLA, as demonstrated by an increase in the water contact angle and water uptake for 11 weeks.

1. Introduction

Poly(lactide) (PLA) is, with difference, one of the most widely used biobased and biodegradable polymers obtained from renewable resources. It has gained significant attention in recent years due to its eco-friendly nature, and currently it can be found in a wide variety of sectors such as packaging, automotive, medical, electronics, construction and building, 3D-printing technology, among others [1–4]. However, PLA is also known for its intrinsic brittleness, which can be a limiting factor in many applications. To overcome or minimize this drawback, several strategies have been proposed.

One of those strategies is blending, which implies the combination of PLA with more ductile polymers in order to increase the ductility of the brittle polymer. To meet this end, several polymers such as poly (ethylene) (PE), poly(propylene) (PP), polyurethanes (PUs), poly (ε-caprolactone) (PCL), poly(butylene adipate-*co*-terephthalate) (PBAT) or poly(ethylene-*co*-glycidyl methacrylate) (PE-*co*-GMA) have been used in blends with PLA to improve its ductile properties [5,6].

Another very interesting option is copolymerization. For example, Mulchandani et al. [7] studied the copolymerization of PLA with polycaprolactone (PCL) in a triblock copolymer, achieving elongation at breaks superior to 500 %. Stefaniak et al. and Coudane et al. [8,9] showed studies where PLA was copolymered with PCL, maleic anhydride (MA), natural rubber, polyethylene glycol (PEG), glycolic acid (GA) or polyhedral oligomeric silsesquioxane (POSS). All those copolymers show improved toughness in comparison with neat PLA.

Fibers have also been used to enhance the mechanical properties of PLA. Glass fibers (GF) and carbon fibers (CF) are some of the most popular ones. Natural fibers are also being studied, such as jute, abaca, hemp or flax fibers [10,11]. In spite of the fact that some of these fibers are quite rigid, they are capable of improving the toughness and general mechanical properties of PLA.

Incorporation of plasticizers is an effective technical solution to provide improved ductility to PLA. In general, plasticizers increase flexibility and toughness. A wide range of plasticizers have been proposed, including monomeric plasticizers such as citrates, malonates, glycerol esters, oligomers of lactic acid, adipates, among others. Polymeric plasticizers have also given interesting properties to PLA. It is worthy to highlight the use of poly(butylene succinate) (PBS), poly (ε-caprolactone) (PCL), poly(butylene succinate-*co*-adipate) (PBSA),

* Corresponding author.
E-mail address: jaugoca@epsa.upv.es (J. Gomez-Caturla).

https://doi.org/10.1016/j.polymer.2023.126522
Received 8 September 2023; Received in revised form 15 November 2023; Accepted 18 November 2023
Available online 22 November 2023

poly(butylene adipate-co-terephthalate) (PBAT), poly(ethylene glycol) (PEG), among others, as polymeric plasticizers for PLA, thus leading to binary/ternary blends with full or partial miscibility, depending on the polymeric plasticizer [12–14]. In general, monomeric plasticizers offer exceptional plasticization performance, but the migration is higher than plasticized PLA formulations containing polymeric plasticizers due to a lower molecule size.

With the aim of broadening the industrial applications of PLA without compromising the biobased nature, new alternative plasticizers are continuously being proposed. Llanes et al. [15] reported the potential of malonate and fumarate isomers as environmentally friendly plasticizers for PLA with a noticeable decrease in glass transition temperature (T_g) from 58 °C (neat PLA) down to 22 °C for the plasticized formulation containing 12 wt% dimethyl fumarate (DMF). Recently, Barandarian et al. [16] have reported the exceptional plasticization efficiency of different cinnamate esters with a noticeable increase in elongation at break from 3.9 % (neat PLA) up to values comprised between 250 and 339 % with 20 wt% cinnamate esters, which was also reflected by a decrease in T_g from 61.7 °C (neat PLA) to values below 40 °C. Ivorra-Martinez et al. [17,18] have shown the extraordinary plasticization efficiency of dibutyl itaconate (DBI) as environmentally friendly plasticizer for PLA. They reported an increase in elongation at break from 4.6 % (neat PLA) up to 322 % with just 10 wt% DBI. Brüster et al. [19] explored the effect of conventional and reactive extrusion (REX) on the plasticization efficiency of terpene-based plasticizers. Other natural terpenes, such as geraniol or linalool have also been reported to possess excellent plasticizing properties, especially when they are reacted with carboxylic acids to form esters [20]. Geraniol esters have shown interesting plasticization properties on poly (3-hydroxybutyrate) as reported in a previous work [21] Nevertheless, despite the solubility parameters of P3HB and geraniol esters suggest good miscibility and hence, good plasticization, the overall plasticization effects of geranyl esters are not exceptional, due to the intrinsic difficulty to plasticize crystalline P3HB.

In this work, PLA is plasticized with a series of biobased plasticizers from geraniol. Specifically, geranyl formate, geranyl acetate, geranyl propionate, geranyl butyrate, geranyl isovalerate and geranyl caproate are tested as plasticizers for PLA in different formulations. Essentially, all those plasticizers possess a similar chemical structure but with different side chain lengths. All these esters are natural-based and thus, they also give an additional environmentally friendly value to PLA. In order to assess the plasticization effect that these esters exert over PLA, as well as other additional properties, mechanical, morphological, thermal, dynamical-thermal-mechanical, colorimetric, chemical and water properties are characterized and evaluated.

2. Materials and methods

2.1. Materials

PLA grade PURAPOL L130 was purchased from Total Corbion PLA (Gorinchem, The Netherlands) with a minimum L-isomer content of 99 % and a melt flow index of 16 g/10 min (ISO 1133-A 210 °C/2.16 kg).

Geranyl acetate (>97 % purity), geranyl propionate (>95 %), geranyl butyrate (>95 %), geranyl isovalerate (>95 %), geranyl formate (>95 %) and geranyl caproate (>95 %) were supplied by Sigma Aldrich (Madrid, Spain). Scheme 1 shows the chemical structure of PLA and all the geranyl esters used in this work as plasticizers, while Table 1 gathers some properties of the selected geraniol esters.

2.2. Theoretical solubility study

When mixing a polymer and a plasticizer, their miscibility is essential to be taken into account. Van Krevelen and Hoftyzer [22], developed a methodology that is very useful to calculate the solubility parameter (δ) of both components by the group contribution method. Equation (1) shows the contribution of the dispersion (δ_d), polar (δ_p) and hydrogen bonding forces (δ_h), to the total solubility parameter (δ), ant their

Table 1
Physical and chemical properties of esters of geraniol used as plasticizers for PLA.

Geranyl ester	density (g cm^{-3})	Molecular weight (g mol^{-1})	Boiling point (°C) at 760 mmHg
Geranyl formate	0.921	182.263	216
Geranyl acetate	0.907	196.290	240–245
Geranyl propionate	0.905	210.317	252–254
Geranyl butyrate	0.894	224.340	242–243
Geranyl isovalerate	0.889	238.371	276–278
Geranyl caproate	0.892	252.398	240

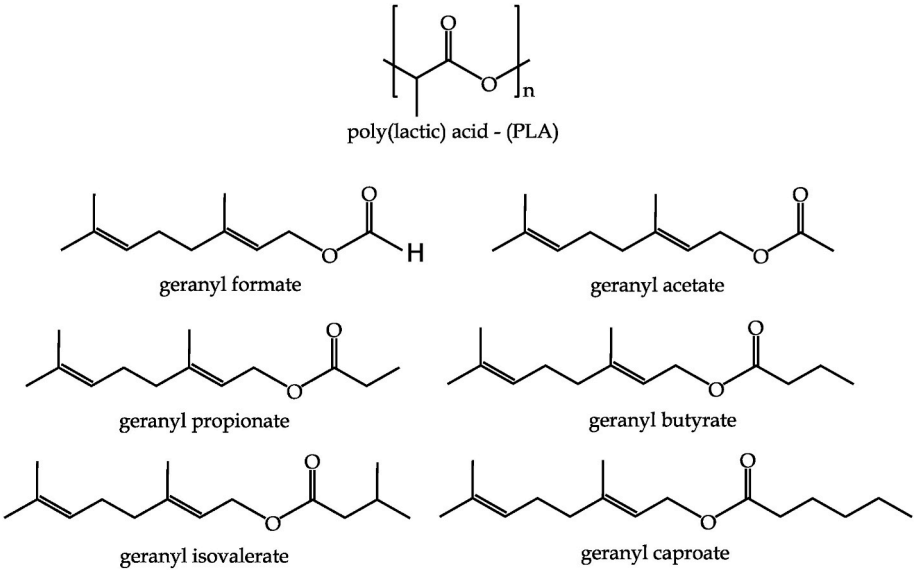

Scheme 1. Chemical structure of poly(lactic) acid and different geranyl-based plasticizers.

relation.

$$\delta^2 = \delta_d^2 + \delta_p^2 + \delta_h^2 \quad (1)$$

Each contribution is calculated according to equations (2)–(4):

$$\delta_d = \frac{\sum F_{di}}{V} \quad (2)$$

$$\delta_p = \frac{\sqrt{\sum F_{pi}^2}}{V} \quad (3)$$

$$\delta_h = \sqrt{\frac{\sum E_{hi}}{V}} \quad (4)$$

Where V [cm^3 mol^{-1}] stands for the molar volume, F_{di} [$(MJ/m^3)^{1/2}$ mol^{-1}] corresponds to the group contributions of the molar attraction constant with regard to the dispersion component, F_{pi} [$(MJ/m^3)^{1/2}$ mol^{-1}] stands for the characteristic molar attraction constants related to the polar component, while E_{hi} [J mol^{-1}] values are representative for the hydrogen bonding energy which are almost constant per structural group.

Table 1 presents all the solubility contributions and the general solubility parameter. The R_a parameter has also been calculated, which is representative for the distance between the solubility coordinates of the studied polymer and the coordinates of the studied plasticizer. If the R_a value is low, it implies a high miscibility between PLA and the plasticizer. If R_a is zero, it means a complete miscibility by both components. There exists a R_a threshold from which the solubility between polymer and plasticizer becomes poor. This value is $R_{0,}$ which is characteristic for each polymer and defines a spherical solubility region for the studied polymer. The center of this sphere is determined by the three solubility parameter contributions of PLA aforementioned. R_a is calculated according to equation (5):

$$R_a = \sqrt{4\cdot\left(\delta_{d_{plast}} - \delta_{d_{PLA}}\right)^2 + \left(\delta_{p_{plast}} - \delta_{p_{PLA}}\right)^2 + \left(\delta_{h_{plast}} - \delta_{h_{PLA}}\right)^2} \quad (5)$$

Another important parameter to give a theoretical idea of the miscibility of a base polymer and a plasticizer, is the relative energy difference (RED). This parameter defines as the ratio between R_a and R_0. In the case of PLA, R_0 is 10.7 $MPa^{1/2}$ (equation (6)) [23]. As the RED value becomes lower, the solubility between the polymer and the plasticizer becomes higher. If RED is equal to one, this means that both elements fall within the threshold of good miscibility, while values superior to 1 suggest poor solubility.

$$RED = \frac{R_a}{R_0} \quad (6)$$

As it is observed in Table 2, all the proposed plasticizers show RED values rather inferior to 1. This implies that all the plasticizers should show good solubility with PLA. Nevertheless, these values are theoretical, thus, they will be corroborated through experimental results.

Table 2
Theoretical solubility parameters of PLA and geraniol esters used as plasticizers.

Material	δ_d ($MPa^{1/2}$)	δ_p ($MPa^{1/2}$)	δ_h ($MPa^{1/2}$)	δ ($MPa^{1/2}$)	Ra ($MPa^{1/2}$)	RED
PLA	15.33	8.44	10.98	20.66	–	–
Geranyl formate	15.16	2.48	5.95	16.47	7.81	0.73
Geranyl acetate	15.98	2.29	5.71	17.12	8.20	0.77
Geranyl propionate	15.88	2.11	5.49	16.93	8.51	0.80
Geranyl butyrate	15.83	1.96	5.29	16.80	8.68	0.81
Geranyl isovalerate	15.63	1.83	5.12	16.55	8.85	0.83
Geranyl caproate	15.90	1.73	4.97	16.75	9.08	0.85

2.3. Processing of plasticized PLA formulations with geraniol esters

PLA was first dried in a hot air drier at 100 °C for 5 h to remove any residual moisture, in order to avoid the hydrolysis of the polymer during processing. Then, PLA was mixed with each plasticizer at a constant proportion of 10 wt%. Neat PLA was also processed without any plasticizer as control material. In order to produce all the formulations, a hot melt manufacturing process was performed in a 15 cc twin-screw micro compounder from Xplore instruments BV (Sittard, The Netherlands). All formulations were prepared using an analytical balance and then they were subjected to a thermal cycle at 100 rpm with a temperature profile of 190 °C for 2 min. Standard samples were obtained in a micro injection moulding unit from Xplore instruments BV (Sittard, The Netherlands) at 190 °C and an injection pressure of 8 bar.

2.4. Mechanical properties

The tensile behavior of the plasticized PLA formulations containing different geraniol esters, was measured using a universal test machine Ibertest ELIB 30 from SAE Ibertest (Madrid, Spain). A 5 kN load cell was used and the measurements followed the ISO 527. Samples were tested at room temperature and the crosshead speed was set at 20 mm min^{-1}. Five different specimens were tested and average values of the main tensile parameters were calculated.

Impact strength of the formulations of PLA with geraniol esters was obtained using notched samples with a Charpy impact pendulum (1-J) from Metrotec S.A. (San Sebastian, Spain), following ISO 179.

Shore D hardness was measured in a 676-D durometer from J. Bot Instruments (Barcelona, Spain) on rectangular samples with dimensions 80 × 10 × 4 mm^3, according to ISO 868:2003.

2.5. Morphological analysis

The morphology of the plasticized PLA blends with geraniol esters was studied by the observation of the fractured surface of broken samples form Charpy test through field emission scanning electron microscopy (FESEM). The samples were first sputtered with a gold-palladium alloy in an EMITECH sputter coating SC7620 model from Quorum Technologies, Ltd. (East Sussex, UK) and then a ZEISS ULTRA 55 microscope from Oxford Instruments (Abingdon, United Kingdom) operated at 2 kV was used to collect FESEM images.

2.6. Thermal properties

In order to study the thermal properties of the plasticized PLA materials, differential scanning calorimetry (DSC) tests were carried out in triplicate using a DSC Mettler-Toledo 821 calorimeter from Mettler-Toledo Inc. (Schwerzenbach, Switzerland) in nitrogen atmosphere using a flow rate of 66 mL min^{-1}. Samples with a weight between 7 and 9 mg were subjected to a dynamic program with three thermal steps: a first heating cycle from 30 °C to 180 °C, a cooling cycle down to 0 °C, and a final second heating cycle from 0 °C to 220 °C. The heating/cooling rate for all the stages was 10 °C/min. The glass transition temperature (T_g) was determined as the inflection point of the baseline change observed in the thermograms, the cold crystallization temperature (T_{cc}) was determined as the peak of the exothermal transition and the melting temperature (T_m) was calculated as the temperature of the peak observed in the characteristic endothermal melting transition observed in the thermograms. The percentage degree of crystallinity (χ_c%), was calculated from equation (7), using the data collected from the second heating step.

$$\chi_c(\%) = \frac{\Delta H_m - \Delta H_{cc}}{\Delta H_m^0 \cdot (1-w)} \cdot 100 \quad (7)$$

Where *1-w* is the weight fraction of PLA in each formulation, ΔH_m is the melting enthalpy of PLA, ΔH_{cc} is the cold crystallization enthalpy and ΔH_m^0 is the melt enthalpy of a 100 % crystalline PLA, which is considered as 93 J/g [24].

Regarding the thermal degradation, it was assessed through thermogravimetric analysis (TGA). TGA characterization was carried out in a TG-DSC2 thermobalance from Mettler-Toledo (Columbus, OH, USA). Specimens with an average weight of 10 mg were subjected to a dynamic heating program from 30 °C to 700 °C at 10 °C/min under air atmosphere was used. All tests were performed in triplicate to obtain reliable results.

2.7. Thermo-mechanical properties

Dynamic mechanical thermal analysis (DMTA) was performed in a Mettler-Toledo DMA1 (Columbus, OH, USA). It worked in single cantilever mode. Samples with dimensions 20 × 6 × 3 mm^3 were used for DMTA characterization. The maximum dynamic deflection at the cantilever was set to 10 μm and the frequency for the sinusoidal deformation was set to 1 Hz. Regarding the heating cycle, tests started at −150 °C and samples were heated up to 100 °C with a heating rate of 2 °C/min.

2.8. Color characterization

Color measurements were carried out using a Konica CM-3600d Colorflex-DIFF2 spectrophotometer from Hunter Associates Laboratory, Inc. (Reston, VA, USA.). L*a*b* color coordinates were measured with L* representing the luminance, a* the color coordinate from green (a* < 0) to red (a* > 0) and b* standing for the color coordinate from blue (b* < 0) to yellow (b* > 0). The yellowing index was calculated as recommended by ASTM E313. 10 measurements were done and the results averaged.

2.9. Water uptake and wetting properties

The water absorption of the samples was assessed by means of the water uptake test following ISO 62:2008. Samples (80 × 10 × 4 mm^3) were immersed in distilled water at room temperature for a period of 11 weeks. Samples were extracted from the water each week and were then dried with paper to measure the mass on an analytical balance AG245 from Mettler-Toledo (Schwerzenbach, Switzerland). Samples were then again immersed in water after the measurement. The weight change was calculated by equation (8):

$$\text{Weight change}(\%) = \frac{W_t - W_0}{W_0} \cdot 100 \quad (8)$$

Where W_t is the weight of the sample after the extraction and W_0 is the initial weight of the sample

Additionally, surface wetting properties were obtained using an optical goniometer EasyDrop Standard model FM140 from KRÜSS GmbH (Hamburg, Germany) equipped with a video capture accessory kit. Double distilled water was used for contact angle measurements using the Drop Shape Analysis SW21; DSA1 software. Flat specimens with dimensions 80 × 10 × 4 mm^3 were used to obtain the water contact angle (θ_w) at room temperature. At least 10 different measurements were done and the obtained θ_w were averaged.

3. Results and discussion

3.1. Mechanical properties

Table 3 gathers all the mechanical parameters relative to the tensile test carried out for all the formulations while Fig. 1 shows the stress-strain curves. Regarding the tensile modulus (E), all plasticizers provoke a clear decrease in this parameter. Neat PLA presents a tensile modulus of 3763 MPa, which is indicative of a relatively high stiffness, while all the plasticized PLA formulations show a decrease in tensile modulus down to 1755–2698 MPa. This indicates certain plasticization exerted by the terpenoids, which promote a decrease in the intensity of the van der Waals forces between polymeric chains, making their interactions weaker [15], leading to a decrease in both tensile modulus and tensile strength. Interestingly, the plasticizers with higher molecular weight (*i.e.* geranyl isovalerate and caproate) provoke a smaller decrease in tensile modulus. This is probably ascribed due to the fact that low molecular weight plasticizers exert a higher lubricant effect over polymeric chains, as they can immerse more easily between them. In a similar manner, tensile strength was also reduced, from a value of 65.8 MPa for neat PLA down to 27–43 MPa for the plasticized PLA formulations. The most remarkable result observed in this analysis is the drastic increase in elongation at break undergone by the plasticized samples. Neat PLA presents an elongation at break of 8.1 %, which is a characteristic behavior of a very brittle polymer with low ductility [25]. On the other hand, the decrease in the intensity of the attraction forces between polymeric chains gives rise to elongation at break values of 300 % for the plasticized PLA with geranyl acetate. The rest of the plasticizers allowed to obtain elongation at break values in the range 235–264 %, which are also impressive numbers, considering the extreme brittleness of neat PLA. This feat again proves the effective plasticization of PLA with geraniol esters and also remarks the good miscibility assessed from the theoretical solubility parameter section.

The Shore D hardness values were also analyzed in Table 3. This parameter follows a similar trend to that observed in the elastic modulus. The addition of the plasticizers reduces the hardness of PLA from 76.6 down to values in the range 37–70, where the highest values correspond to the plasticizers with the highest molecular weight. This fact is also ascribed to an increased chain mobility in the polymer as a result of the lubricant effect of the plasticizer.

On the contrary to hardness, impact strength (which is indicative of toughness) was increased thanks to the incorporation of the geraniol ester-based plasticizers into PLA. PLA showed a value of 1.1 kJ m^{-2}, while the rest of the samples exhibited values between 2.2 and 6.1 kJ m^{-2}, thus indicating a clear improvement in toughness. Again, geranyl acetate together with geranyl formate leads to obtain the highest impact strength, similar to the elongation at break trend, which could be a consequence of a better miscibility with PLA, as it was observed in the theoretical solubility study, where the RED value was the lowest for geranyl acetate and geranyl formate, thus proving the superior mechanical properties.

3.2. Morphological analysis

In order to provide support to the mechanical results presented in the previous section, FESEM morphological analysis was carried out over the fractured surface of Charpy impact test specimens. Fig. 2 shows the FESEM images of all the formulations at 1500 × magnification. Fig. 2a corresponds to neat PLA, and clearly shows the typical flat surface with very little roughness, which is representative for quite a brittle behavior with absence of plastic deformation [26]. Totally in contrast with this behavior, all the rest of plasticized PLA samples exhibit clear signs of plasticization. This is denoted by a rough and cavernous surface with even some filament-like formations [27]. This effect seems to be especially visible in Fig. 2b and c, which corresponds to plasticized PLA with geranyl formate and geranyl acetate respectively, which are the

Table 3
Main mechanical parameters obtained for each one of the plasticized PLA formulations.

Code	E (MPa)	σ_{max} (MPa)	ε_b (%)	Shore D Hardness	Impact Strength (kJ/m^2)
PLA	3763 ± 38	65.6 ± 2.0	8.1 ± 0.2	76.6 ± 1.3	1.1 ± 0.2
PLA/10FORMATE	1755 ± 45	26.8 ± 3.4	262.4 ± 5.3	43.5 ± 1.5	5.2 ± 0.2
PLA/10ACETATE	1509 ± 29	30.4 ± 3.8	301.9 ± 3.5	63.3 ± 2.1	6.1 ± 0.4
PLA/10PROPIONATE	1865 ± 46	37.2 ± 2.3	264.3 ± 4.0	45.5 ± 1.9	2.2 ± 0.1
PLA/10BUTIRATE	2239 ± 41	32.3 ± 1.8	250.0 ± 5.7	37.8 ± 2.1	2.3 ± 0.2
PLA/10ISOVALERATE	2698 ± 32	43.2 ± 3.1	237.6 ± 2.2	68.9 ± 1.4	3.0 ± 0.2
PLA/10CAPROATE	2341 ± 37	41.6 ± 3.4	235.3 ± 6.3	70.0 ± 1.9	2.4 ± 0.4

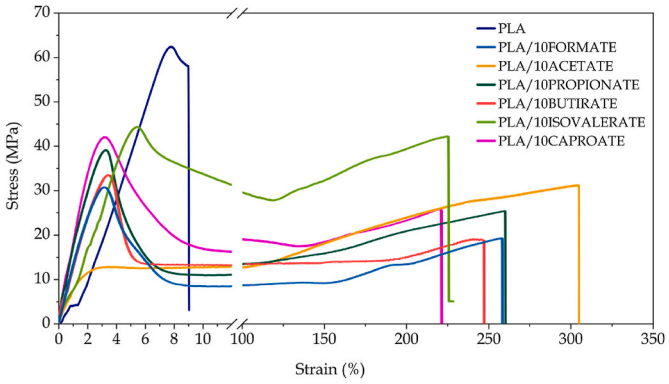

Fig. 1. Stress-Strain curves obtained from the mechanical tensile test for the developed plasticized PLA formulations.

plasticized formulations with the highest elongation at break and impact strength as mentioned above. These results perfectly match the findings observed in the previous section, with all the plasticized samples presenting an effective visible plasticization and without signs of phase separation. This latter fact is also in total accordance with the theoretical miscibility results, which shown that all the plasticizers offered good compatibility with PLA, especially geranyl formate, which presented the lowest RED value (0.73), indicative of superior miscibility with PLA.

3.3. Thermal properties

Fig. 3 shows all the thermograms that correspond to the second heating cycle obtained by differential scanning calorimetry (DSC), for neat PLA and all the plasticized formulations with geraniol esters. Table 4 gathers the main thermal parameters that have been extracted from those thermograms. Neat PLA exhibits a typical glass transition temperature (T_g) of 61.6 °C [28]. All the used plasticizers clearly decrease T_g down to values in the range 46–56 °C, which is indicative of an effective plasticization, especially in the case of PLA with geranyl caproate, which achieves a T_g value of 45 °C. This is ascribed to an increase in the mobility of the polymeric chains in the amorphous region of PLA. Very similar values were reported by Maiza et al. [29], in formulations of plasticized PLA with citrate esters. This fact demonstrates the effectiveness of these new natural plasticizers in comparison with

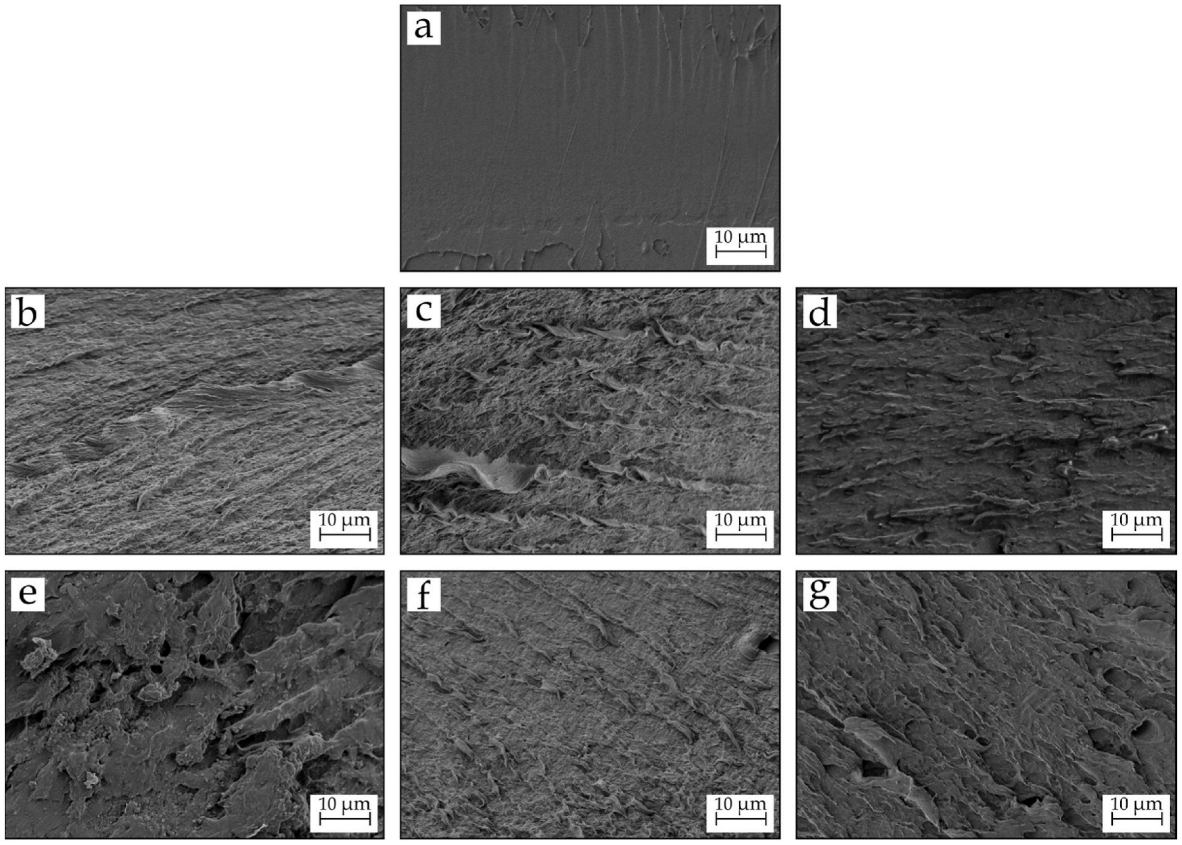

Fig. 2. FESEM images at 1500 × magnification for each one of the plasticized PLA formulations: (a) PLA, (b) PLA/10FORMATE, (c) PLA/10ACETATE, (d) PLA/10PROPIONATE, (e) PLA/10BUTYRATE, (f) PLA/10ISOVALERATE and (g) PLA/10CAPROATE.

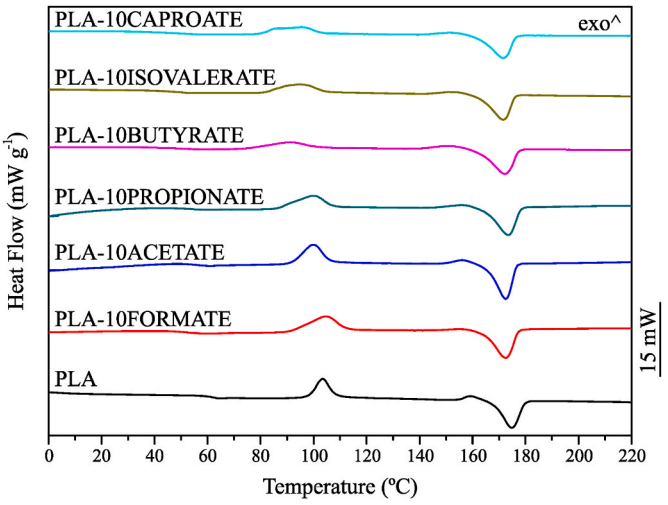

Fig. 3. Second heating cycle thermograms obtained by DSC of all the plasticized PLA formulations.

most conventional PLA plasticizers such as TEC and ATBC. A similar trend is observed for the cold crystallization temperature peak (T_{cc}), which is shifted from a value of 102 °C (neat PLA) down to values of 91–100 °C in plasticized PLA formulations. This is also related to an increased chain mobility of the polymer as a result of the plasticizing effect, which makes these chains easier to rearrange into a crystalline formation and makes them more readily to pack [15]. The melting peak temperature does not suffer a noticeable change, as it fluctuates in the 171–173 °C range, although it seems that the plasticizers slightly decrease it. Regarding crystallinity, only geranyl butyrate increases it up to 39 %, in comparison with 29 % of neat PLA. This is due to the plasticizer increasing the concentration of crystal growth nuclei and thus catalyzing the crystallization of the polymer [30]. However, this effect was not observed for the rest of the plasticizers. All in all, these results prove a clear plasticization effect exerted by the geranyl esters.

Additionally to DSC analysis, the thermal degradation of all the plasticized PLA formulations with geraniol esters was studied by means of thermogravimetric analysis (TGA), and its first derivative (DTG). Fig. 4 shows the TGA thermograms for each one of the developed formulations as well as the first derivative (DTG), which allows to better determine the maximum degradation rate. At first glance, it can be seen that neat PLA presents a typical one-step thermal degradation profile due to chain scission, with an onset degradation temperature (temperature at which the mass loss is 5 %) of 357 °C and a maximum degradation rate temperature of 380 °C [31]. It can be seen that when plasticizers are added to PLA, the thermodegradation profile becomes a two-step process. The first process, occurring between 200 and 300 °C is ascribed to plasticizer volatilization, leading to a decrease in the onset temperature down to values in the 233–279 °C range [32]. As it can be seen, the mass loss for all geraniol ester-based plasticizers is close to 10 wt% in this first mass loss step, which is indicating very low plasticizer volatilization during processing. Interestingly, the onset degradation temperature becomes higher as the molecular weight of the plasticizer also increases. Thus, while geranyl formate (the plasticizer with the lowest molecular weight and chain length) presents an onset degradation temperature of 233 °C, geranyl caproate (the plasticizer with the highest molecular weight and largest chain length) presents a value of 279 °C for this parameter. This is obviously ascribed to the boiling point of the plasticizers, which becomes greater the higher their molecular weight is, as it is observed in Table 1. Regarding the maximum degradation rate temperature, it does not vary in great measure in spite of introducing the plasticizers, although it is slightly lower than the value presented by neat PLA. This is the expected behavior since the second degradation steps is ascribed to PLA degradation, once the plasticizer has been removed at lower temperature. Similar results were observed by Gálvez et al. [33], in blends of PLA plasticized with acetyl tributyl citrate (ATBC), where the maximum degradation rate temperature maintained in the range 364–370 °C. Finally, the residual mass is almost 0 in all the developed blends, which was an expected result as theoretically, at 700 °C all the components present in this study should be completely decomposed. The effect of the different geraniol ester-based plasticizers on thermal degradation can also be seen in Table 5 which gathers the main thermal degradation parameters.

Table 4
Main thermal parameters extracted from the DSC thermograms.

Code	T_g (°C)	T_{cc} (°C)	T_m (°C)	ΔH_{cc} (J g^{-1})	ΔH_m (J g^{-1})	χ_c (%)
PLA	61.6 ± 2.2	102.8 ± 1.1	173.3 ± 1.2	24.3 ± 0.8	51.7 ± 0.2	29.4 ± 0.3
PLA-10FORMATE	51.3 ± 3.1	104.6 ± 1.4	172.4 ± 1.4	27.2 ± 1.1	39.3 ± 0.7	14.5 ± 1.2
PLA-10ACETATE	55.9 ± 1.3	99.8 ± 1.1	172.6 ± 1.5	25.3 ± 1.2	43.5 ± 0.8	21.7 ± 1.1
PLA-10PROPIONATE	54.3 ± 2.0	99.8 ± 1.5	173.4 ± 2.0	26.9 ± 0.9	46.0 ± 1.2	22.8 ± 1.9
PLA-10BUTYRATE	47.6 ± 2.1	91.2 ± 1.4	172.2 ± 2.1	15.5 ± 0.7	48.3 ± 1.1	39.2 ± 1.5
PLA-10ISOVALERATE	50.4 ± 3.4	95.1 ± 1.3	171.6 ± 1.4	22.2 ± 0.7	46.5 ± 1.2	29.0 ± 1.9
PLA-10CAPROATE	45.9 ± 1.8	95.3 ± 1.4	171.5 ± 1.8	21.7 ± 0.9	43.9 ± 0.8	26.5 ± 1.3

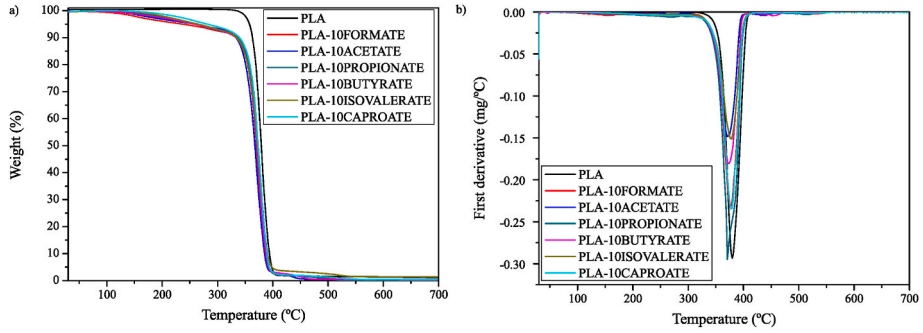

Fig. 4. a) Thermogravimetric analysis (TGA) thermograms of the plasticized PLA formulations with geraniol esters, (b) first derivative of the TGA of all the developed formulations.

Table 5
Main thermal parameters extracted from the TGA and DTG analyses.

Code	$T_{5\%}$ (°C)	T_{max} (°C)	*Residue*
PLA	357.9 ± 2.0	380.0 ± 1.1	0.1 ± 0.1
PLA-10FORMATE	233.3 ± 3.2	375.9 ± 1.4	0.2 ± 0.1
PLA-10ACETATE	260.6 ± 3.3	370.8 ± 1.1	0.3 ± 0.1
PLA-10PROPIONATE	260.7 ± 3.0	378.5 ± 1.5	0.2 ± 0.1
PLA-10BUTYRATE	261.1 ± 3.1	373.3 ± 1.4	0.4 ± 0.1
PLA-10ISOVALERATE	266.5 ± 3.4	377.5 ± 1.3	0.3 ± 0.1
PLA-10CAPROATE	279.8 ± 3.8	378.1 ± 1.4	0.5 ± 0.1

3.4. Thermo-mechanical properties

Dynamic mechanical thermal analysis (DMTA) allowed to obtain the thermomechanical properties of the developed PLA-based formulations. Fig. 5 shows the evolution of the storage modulus (E') and the dynamic damping factor (tan δ) in function of temperature for all the plasticized PLA formulations. Regarding the storage modulus, neat PLA presents an almost constant modulus (2361 at −20 °C) until it reaches 60 °C, when it suffers a drastic decrease (almost three fold) in the temperature range comprised between 60 and 70 °C. This is ascribed to the glass transition of the polymer occurring in this temperature range. After the glass transition, at approximately 80 °C, the storage modulus increases up to values close to 50 MPa. This last increase is related to the cold crystallization process of the polymer, as an increase in crystallinity is associated with an increase in stiffness, and hence, the storage modulus is increased. It is clearly observable that the plasticized samples see their sudden decrease related to the glass transition moved to lower temperatures, as it was expected from DSC results. The same effect occurs with the increase in storage modulus related to the cold crystallization temperature, which is also shifted towards lower temperatures in comparison with neat PLA. This is ascribed to an enhancement of chain mobility in the amorphous regions of PLA exerted by the plasticizers. The glass transition temperature (T_g) was calculated according to the peaks observed in the tan δ graphs. Neat PLA presents a T_g of 65 °C, while the rest of the samples oscillate between 41 and 45 °C, which is a considerable decrease in this parameter (see Table 6). This effect is an indicative of a great efficiency of these plasticizers over PLA. These results perfectly match the ones reported in DSC analysis. Moreover, the glass transition values are in accordance with the miscibility parameters observed in the theoretical solubility study, where geranyl formate exhibited the lowest RED value, as it is the case with the glass transition temperature (41.1 °C). Additionally, it can be observed that the height of the tan δ decreased from a value of 3.42 for neat PLA down to values between 1.85 and 2.61 for the plasticized samples. This effect was also reported by Ivorra-Martinez et al. [34] and Maiza et al. [35], who reported a decrease in the height of the tan δ peak in dibutyl itaconate (DBI) and other environmentally friendly plasticized PLA formulations. This effect often originates also a peak widening, that indicates a greater glass transition temperature range, which allows the polymer to behave in a rubber-like manner at larger temperature ranges.

Table 6
Main thermal parameters obtained from dynamic-mechanical thermal analysis (DMTA).

Code	T_g (°C)	tan δ peak height	*E'* at −20 °C (MPa)	*E'* at 100 °C (MPa)
PLA	65.0 ± 0.8	3.42 ± 0.3	2361 ± 25	45 ± 13
PLA-10FORMATE	41.1 ± 0.6	1.85 ± 0.2	2038 ± 33	47 ± 22
PLA-10ACETATE	43.1 ± 0.7	2.38 ± 0.4	2074 ± 14	50 ± 25
PLA-10PROPIONATE	42.7 ± 0.4	2.39 ± 0.3	2278 ± 41	49 ± 31
PLA-10BUTYRATE	43.5 ± 0.7	2.41 ± 0.2	2176 ± 37	68 ± 17
PLA-10ISOVALERATE	43.6 ± 0.5	2.59 ± 0.3	2268 ± 49	48 ± 28
PLA-10CAPROATE	45.1 ± 0.4	2.61 ± 0.3	2291 ± 52	52 ± 25

3.5. Color characterization

The visual appearance of the blends was assessed by colorimetric analysis, as this aspect is essential for the impression a product produced with those materials makes in the customer. Table 7 gathers the main CieL*a*b* colorimetric parameters of neat PLA and the plasticized PLA samples while Fig. 6 shows the visual appearance of all the studied formulations. L* stands for luminance, and it indicates the brightness of the color of the samples, the higher this parameter is, the closer the color is to pure white. It can be observed that all samples present a very similar luminance, with a range between 36 and 38. This is ascribed to the typical white transparent color of PLA, which is not greatly affected by the introduction of plasticizers in the blends, as it can be corroborated by Fig. 7. The color coordinate a* indicates green (negative) or red (positive) tonalities. In this case all samples present very similar negative values (between −0.3 and −0.8). These values are close to 0 as the colors presented by the samples are very close to white. The color coordinate

Table 7
CieLab color coordinates and yellow index of the plasticized PLA samples with different geraniol esters.

Code	L*	a*	b*	YI
PLA	38.1 ± 0.1	−0.3 ± 0.1	1.2 ± 0.2	4.6 ± 0.3
PLA-10FORMATE	37.8 ± 0.1	−0.6 ± 0.1	2.2 ± 0.1	8.0 ± 0.3
PLA-10ACETATE	36.6 ± 0.1	−0.4 ± 0.1	2.1 ± 0.1	8.1 ± 0.5
PLA-10PROPIONATE	37.8 ± 0.1	−0.7 ± 0.1	2.8 ± 0.1	10.2 ± 0.3
PLA-10BUTIRATE	37.1 ± 0.1	−0.6 ± 0.1	2.9 ± 0.1	11.0 ± 0.3
PLA-10ISOVALERATE	38.5 ± 0.1	−0.4 ± 0.2	1.9 ± 0.1	7.0 ± 0.4
PLA-10CAPROATE	38.2 ± 0.1	−0.8 ± 0.1	2.8 ± 0.1	10.4 ± 0.1

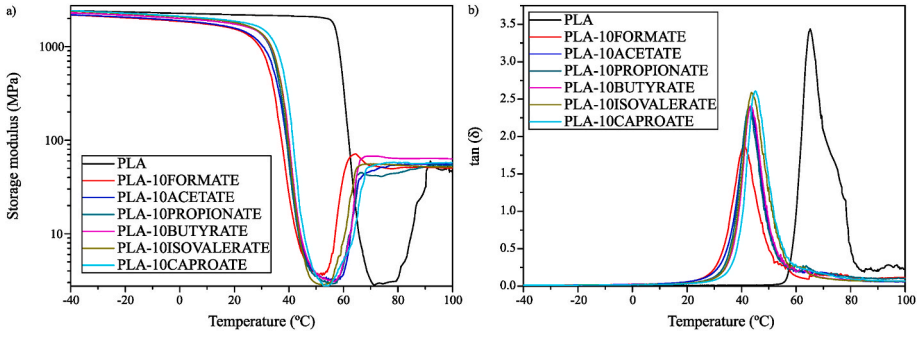

Fig. 5. a) Storage modulus (E′) evolution *versus* temperature of all the plasticized PLA formulations, (b) dynamic damping factor (tan δ) evolution *versus* temperature of all the plasticized PLA formulations.

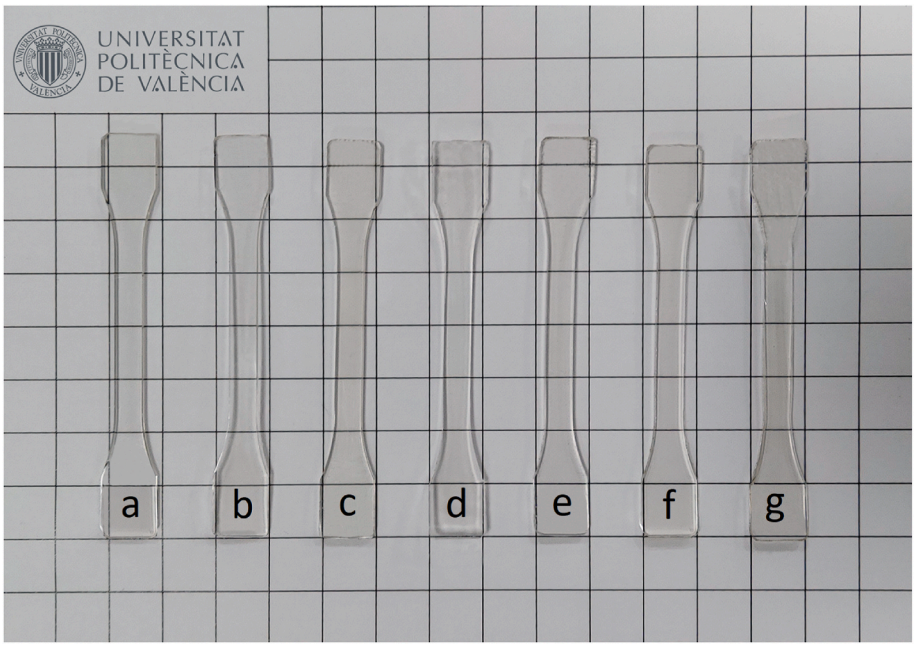

Fig. 6. Visual aspect of the developed samples: (a) PLA, (b) PLA/10FORMATE, (c) PLA/10ACETATE, (d) PLA/10PROPIONATE, (e) PLA/10BUTYRATE, (f) PLA/10ISOVALERATE and (g) PLA/10CAPROATE.

b* indicates blue (negative) of yellow (positive) shades. As expected, all samples present positive values due to a certain approach to yellow. The plasticizers seem to increase this value, as they turn the color of PLA towards a higher yellow degree, as it will be discussed with the following parameter. Finally, the yellowness index (YI), which indicates how the color is changed from white to yellow, seems to increase as a result of the incorporation of the plasticizers into PLA. This can be slightly appreciated in Fig. 7, especially in sample *g*, which is plasticized with geranyl caproate and seems to present an opaquer color. Nonetheless, all the samples are clearly transparent. Similar results and visual appearance were observed for PLA samples plasticized with ATBC and PEG [36], although the samples presented here preserve even better the natural color of PLA.

3.6. Water uptake properties

Fig. 7 shows the evolution of water absorption over time for neat PLA and all the plasticized samples after being immersed in distilled water for 11 weeks. As it can be seen, neat PLA presents the lowest water absorption profile of all the presented materials, with a maximum water absorption of approximately 0.38 wt% of water with relation to the initial weight of the sample. This fact indicates certain hydrophobic behavior in PLA. A similar behavior was observed by Dominguez-Candela et al. [37]. When the different plasticizers are added into PLA, its water absorption slightly increases, especially in the case of geranyl formate. All the plasticizers achieve maximum water uptake values at 11 weeks of approximately 0.45 wt%, which could be ascribed to the plasticization effect that increases the free volume between the polymeric chains. After all, the plasticizers weaken the intermolecular attraction forces between PLA chains, thus increasing water diffusion within the polymer [38]. All those plasticizers provide a similar water absorption capacity to PLA, without much variability from the neat polymer. This could be ascribed to the fact that all of them possess a similar chemical structure, which does not possess great polarity, as there is only one oxygen-based functionalization (ester group), while the rest of the chemical structure is formed by C–H bonds, which are essentially non-polar. Interestingly, geranyl formate allows PLA to absorb a higher degree of water (up to 0.8 wt%) in comparison to the rest of the samples. This could be due to the fact that it is the plasticizer

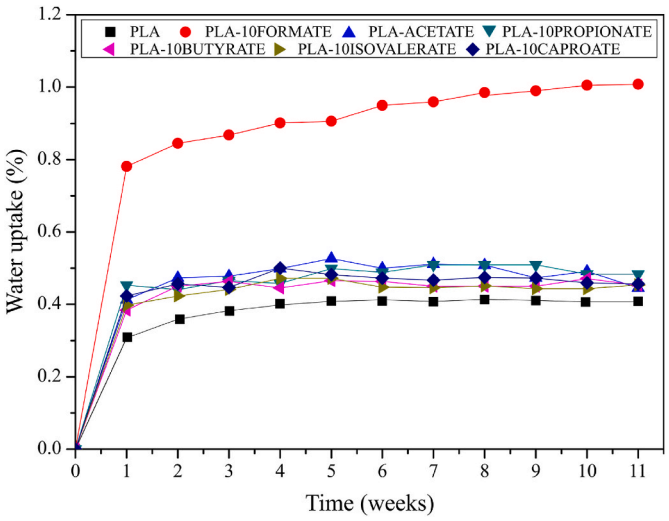

Fig. 7. Evolution of the water absorption of neat PLA and plasticized PLA formulations with geraniol ester-based plasticizers.E.

with the lowest molecular weight among the studied ones, which accounts for a smaller molecule which could better insert between PLA chains, thus increasing in a slightly higher degree the free volume between them. This would translate in a higher capability to accept water in the internal structure of the polymer. Nonetheless, the general water absorption of the herein studied blends is quite low in comparison with other materials that are more compromised by this property, as wood plastic composites, which can achieve water uptakes of more than 10 wt % [39].

3.7. Wetting properties

Water contact angle measurements were taken in order to complement the water uptake results. In this case, the behavior of the materials after short-time exposition to water is studied. Fig. 8 shows the visual appearance of distilled water drops over the surface of samples from

each one of the materials as well as the contact angle they form with the flat surface. It can be observed in Fig. 8a that neat PLA presents a contact angle of 76.4°, which is indicative of a rather hydrophobic behavior, as this value is relatively close to 90°, which is the "highly hydrophobic" threshold [40]. A similar result was obtained by Jordá-Vilaplana et al. [40] for neat PLA. The plasticized samples present a slightly superior hydrophilic behavior, especially the sample with geranyl formate, which presents a contact angle of approximately 70°. The used plasticizers possess oxygen-based functionality, which increase the polarity of the PLA/plasticizer blends. These plasticizers present a non-polar fraction (C–H bonds) and a polar fraction (ester groups), therefore, the plasticizers with longer chain length, such as geranyl caproate, provide less polarity to PLA due to it having a higher non-polar fraction (longer C–H chains) and thus, the contact angle observed is superior to the angle observed for geranyl formate or geranyl acetate [41]. The contact angles of the samples with geranyl acetate, propionate, butyrate, isovalerate and caproate range from 72 to 74°, which are still lower than that of neat PLA. These results are in accordance with the results obtained in the water uptake section previously described.

4. Conclusions

This work has shown that several geraniol esters with different chain lengths (geranyl formate, acetate, propionate, butyrate, isovalerate and caproate) can effectively plasticize poly(lactic acid) (PLA), providing excellent results in terms of ductility. The mechanical properties results showed that all the plasticizers drastically increased elongation at break from 8 % up to values in the range 230–300 %, which are quite impressive results considering the poor ductility of neat PLA. Geranyl formate showed the highest elongation at break. Those results were confirmed by FESEM images, which exhibited clear signs of plasticization in the fractured surface of all the plasticized samples. Regarding their thermal behavior, DSC analysis showed a decrease of approximately 10 °C in the glass transition temperature, attributed to an increase in the chain mobility of the amorphous phase of PLA, thus, demonstrating an excellent plasticization effect. Thermogravimetric analysis (TGA) clearly indicated a slight reduction in the thermal stability of the blends due to the high volatility of the plasticizer in the temperature range 200–300 °C and DMTA results again pointed out a decrease in the glass transition temperature. Water properties revealed a slight increase in the water absorption of PLA, especially in the case of geranyl formate, which, due to the presence of oxygen-based ester functionalization in its structure, increased the polarity of the formulations. All in all, this work presents a new alternative to traditional plasticizers such as poly(ethylene glycol) (PEG) or triethyl citrate (TEC), which are additionally environmentally friendly.

CRediT authorship contribution statement

J. Gomez-Caturla: Investigation, Writing – original draft, Writing – review & editing. **J. Ivorra-Martinez:** Software, Methodology. **R. Tejada-Oliveros:** Visualization, Formal analysis, Writing – original draft. **V. Moreno:** Supervision, Writing – review & editing, Validation, Project administration. **D. Garcia-Garcia:** Conceptualization, Data curation, Supervision. **R. Balart:** Investigation, Visualization, Supervision.

Declaration of competing interest

The authors declare that they have no known competing financial interests or personal relationships that could have appeared to influence the work reported in this paper.

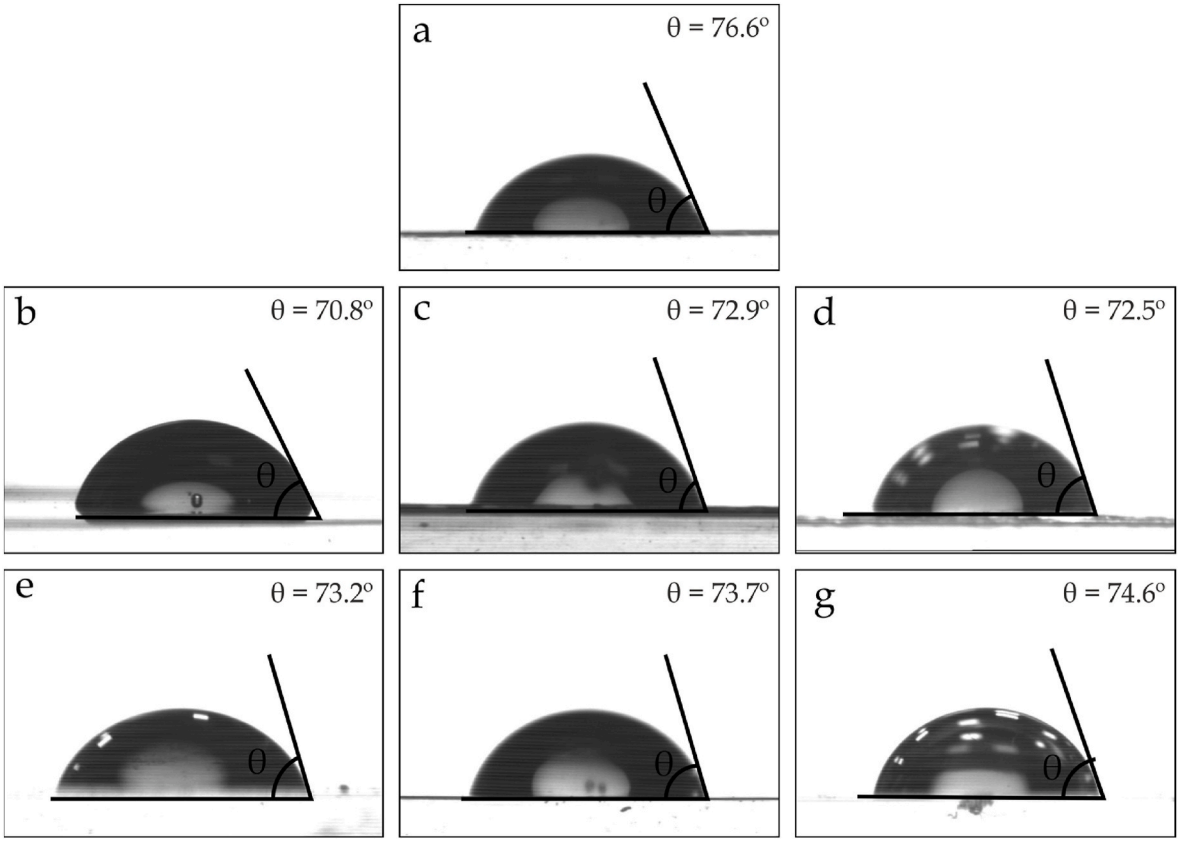

Fig. 8. Contact angle measurements of: (a) PLA, (b) PLA/10FORMATE, (c) PLA/10ACETATE, (d) PLA/10PROPIONATE, (e) PLA/10BUTYRATE, (f) PLA/10ISOVALERATE and (g) PLA/10CAPROATE.

Data availability

Data will be made available on request.

Acknowledgements

This research is a part of the grant PID2020-116496RB-C22, funded by MCIN/AEI/10.13039/501100011033 and the grant TED2021-131762A-I00, funded by MCIN/AEI/10.13039/501100011033 and by the European Union "NextGenerationEU"/PRTR. Authors also thank Generalitat Valenciana-GVA for funding this research through the grant numbers AICO/2021/025 and CIGE/2021/094. Funded with Aid for First Research Projects (PAID-06-22), Vice-rectorate for Research of the Universitat Politècnica de València (UPV). R.T.-O. wishes to thank UPV for the grant received though the PAID-01-20 program. J. I.-M. wants to thank FPU19/01759 grant funded by MCIN/AEI/10.13039/501100011033 and by ESF Investing in your future. J. G.-C. wants to thank FPU20/01732 grant funded by MCIN/AEI/10.13039/501100011033 and by ESF Investing in your future. V. M. thanks Generalitat Valenciana - GVA for funding a postdoc position through the APOSTD program co-funded by ESF Investing in your future, grant number CIAPOS/2021/67. Microscopy Services at UPV are also acknowledged by their help in collecting and analyzing images.

References

[1] C. Aversa, M. Barletta, G. Cappiello, A. Gisario, Compatibilization strategies and analysis of morphological features of poly (butylene adipate-co-terephthalate) (PBAT)/poly (lactic acid) PLA blends: a state-of-art review, Eur. Polym. J. (2022), 111304.

[2] H. Saniei, S. Mousavi, Surface modification of PLA 3D-printed implants by electrospinning with enhanced bioactivity and cell affinity, Polymer 196 (2020), 122467.

[3] S. Singh, G. Singh, C. Prakash, S. Ramakrishna, L. Lamberti, C.I. Pruncu, 3D printed biodegradable composites: an insight into mechanical properties of PLA/chitosan scaffold, Polym. Test. 89 (2020), 106722.

[4] S. Bhagia, K. Bornani, R. Agrawal, A. Satlewal, J. Ďurkovič, R. Lagaňa, M. Bhagia, C.G. Yoo, X. Zhao, V. Kunc, Critical review of FDM 3D printing of PLA biocomposites filled with biomass resources, characterization, biodegradability, upcycling and opportunities for biorefineries, Appl. Mater. Today 24 (2021), 101078.

[5] S. Moradi, J.K. Yeganeh, Highly toughened poly (lactic acid)(PLA) prepared through melt blending with ethylene-co-vinyl acetate (EVA) copolymer and simultaneous addition of hydrophilic silica nanoparticles and block copolymer compatibilizer, Polym. Test. 91 (2020), 106735.

[6] S.M. Bhasney, A. Kumar, V. Katiyar, Microcrystalline cellulose, polylactic acid and polypropylene biocomposites and its morphological, mechanical, thermal and rheological properties, Compos. B Eng. 184 (2020), 107717.

[7] N. Mulchandani, K. Masutani, S. Kumar, H. Yamane, S. Sakurai, Y. Kimura, V. Katiyar, Toughened PLA-b-PCL-b-PLA triblock copolymer based biomaterials: effect of self-assembled nanostructure and stereocomplexation on the mechanical properties, Polym. Chem. 12 (26) (2021) 3806–3824.

[8] K. Stefaniak, A. Masek, Green copolymers based on poly (lactic acid)—short review, Materials 14 (18) (2021) 5254.

[9] J. Coudane, H. Van Den Berghe, J. Mouton, X. Garric, B. Nottelet, Poly (lactic acid)-based graft copolymers: syntheses strategies and improvement of properties for biomedical and environmentally friendly applications: a review, Molecules 27 (13) (2022) 4135.

[10] G. Wang, D. Zhang, G. Wan, B. Li, G. Zhao, Glass fiber reinforced PLA composite with enhanced mechanical properties, thermal behavior, and foaming ability, Polymer 181 (2019), 121803.

[11] Y.E. Belarbi, S. Guessasma, S. Belhabib, F. Benmahiddine, A.E.A. Hamami, Effect of printing parameters on mechanical behaviour of PLA-flax printed structures by fused deposition modelling, Materials 14 (19) (2021) 5883.

[12] S. Cesur, S. Ulag, L. Ozak, A. Gumussoy, S. Arslan, B.K. Yilmaz, N. Ekren, M. Agirbasli, O. Gunduz, Production and characterization of elastomeric cardiac tissue-like patches for Myocardial Tissue Engineering, Polym. Test. 90 (2020), 106613.

[13] B. Palai, S. Mohanty, S.K. Nayak, Synergistic effect of polylactic acid (PLA) and Poly (butylene succinate-co-adipate)(PBSA) based sustainable, reactive, super toughened eco-composite blown films for flexible packaging applications, Polym. Test. 83 (2020), 106130.

[14] M. Hernández-López, Z.N. Correa-Pacheco, S. Bautista-Baños, L. Zavaleta-Avejar, J. J. Benítez-Jiménez, M.A. Sabino-Gutiérrez, P. Ortega-Gudiño, Bio-based composite fibers from pine essential oil and PLA/PBAT polymer blend, Morphological, physicochemical, thermal and mechanical characterization, Materials Chemistry and Physics 234 (2019) 345–353.

[15] L.C. Llanes, S.H. Clasen, A.T. Pires, I.P. Gross, Mechanical and thermal properties of poly (lactic acid) plasticized with dibutyl maleate and fumarate isomers: promising alternatives as biodegradable plasticizers, Eur. Polym. J. 142 (2021), 110112.

[16] A. Barandiaran, J. Gomez-Caturla, J. Ivorra-Martinez, D. Lascano, M.A. Selles, V. Moreno, O. Fenollar, Esters of Cinnamic Acid as Green Plasticizers for Polylactide Formulations with Improved Ductility, Macromolecular Materials and Engineering, 2023, 2300022.

[17] J. Ivorra-Martinez, M.A. Peydro, J. Gomez-Caturla, T. Boronat, R. Balart, The Potential of an Itaconic Acid Diester as Environmentally Friendly Plasticizer for Injection-Molded Polylactide Parts, Macromolecular Materials and Engineering, 2022, 2200360.

[18] J. Ivorra-Martinez, J. Gomez-Caturla, N. Montanes, L. Quiles-Carrillo, F. Dominici, D. Puglia, L. Torre, Effect of dibutyl itaconate on plasticization efficiency of a REX processed polylactide with peroxides, Polym. Test. (2023), 108059.

[19] B. Brüster, Y.-O. Adjoua, R. Dieden, P. Grysan, C.E. Federico, V. Berthé, F. Addiego, Plasticization of polylactide with myrcene and limonene as bio-based plasticizers: conventional vs. reactive extrusion, Polymers 11 (8) (2019) 1363.

[20] L. da Silva Corrêa, R.O. Henriques, J.V. Rios, L.A. Lerin, D. de Oliveira, A. Furigo, Lipase-catalyzed esterification of geraniol and citronellol for the synthesis of terpenic esters, Appl. Biochem. Biotechnol. 190 (2020) 574–583.

[21] C. Mangeon, L. Michely, A.n. Rios de Anda, F. Thevenieau, E. Renard, V. Langlois, Natural terpenes used as plasticizers for poly (3-hydroxybutyrate), ACS Sustain. Chem. Eng. 6 (12) (2018) 16160–16168.

[22] D.W. Van Krevelen, K. Te Nijenhuis, Properties of Polymers: Their Correlation with Chemical Structure; Their Numerical Estimation and Prediction from Additive Group Contributions, Elsevier, 2009.

[23] R.A. Auras, L.-T. Lim, S.E. Selke, H. Tsuji, Poly (Lactic Acid): Synthesis, Structures, Properties, Processing, and Applications, John Wiley & Sons, 2011.

[24] S. Shankar, L.-F. Wang, J.-W. Rhim, Incorporation of zinc oxide nanoparticles improved the mechanical, water vapor barrier, UV-light barrier, and antibacterial properties of PLA-based nanocomposite films, Mater. Sci. Eng. C 93 (2018) 289–298.

[25] M. Murariu, A.D.S. Ferreira, M. Pluta, L. Bonnaud, M. Alexandre, P. Dubois, Polylactide (PLA)–CaSO4 composites toughened with low molecular weight and polymeric ester-like plasticizers and related performances, Eur. Polym. J. 44 (11) (2008) 3842–3852.

[26] A. Bagheri, M.S.A. Parast, A. Kami, M. Azadi, V. Asghari, Fatigue testing on rotary friction-welded joints between solid ABS and 3D-printed PLA and ABS, Eur. J. Mech. Solid. 96 (2022), 104713.

[27] J. Gomez-Caturla, I. Dominguez-Candela, M.P. Medina-Casas, J. Ivorra-Martinez, V. Moreno, R. Balart, D. Garcia-Garcia, Improvement of Poly (Lactide) Ductile Properties by Plasticization with Biobased Tartaric Acid Ester, Macromolecular Materials and Engineering, 2023, 2200694.

[28] A. Carbonell-Verdu, D. Garcia-Garcia, F. Dominici, L. Torre, L. Sanchez-Nacher, R. Balart, PLA films with improved flexibility properties by using maleinized cottonseed oil, Eur. Polym. J. 91 (2017) 248–259.

[29] M. Maiza, M.T. Benaniba, V. Massardier-Nageotte, Plasticizing effects of citrate esters on properties of poly (lactic acid), J. Polym. Eng. 36 (4) (2016) 371–380.

[30] C.M. Clarkson, S.M.E.A. Azrak, G.T. Schueneman, J.F. Snyder, J.P. Youngblood, Crystallization kinetics and morphology of small concentrations of cellulose nanofibrils (CNFs) and cellulose nanocrystals (CNCs) melt-compounded into poly (lactic acid)(PLA) with plasticizer, Polymer 187 (2020), 122101.

[31] M. Oliveira, E. Santos, A. Araújo, G.J. Fechine, A.V. Machado, G. Botelho, The role of shear and stabilizer on PLA degradation, Polym. Test. 51 (2016) 109–116.

[32] P. Brdlík, M. Borůvka, L. Běhálek, P. Lenfeld, Biodegradation of poly (lactic acid) biocomposites under controlled composting conditions and freshwater biotope, Polymers 13 (4) (2021) 594.

[33] J. Gálvez, J.P. Correa Aguirre, M.A. Hidalgo Salazar, B. Vera Mondragón, E. Wagner, C. Caicedo, Effect of extrusion screw speed and plasticizer proportions on the rheological, thermal, mechanical, morphological and superficial properties of PLA, Polymers 12 (9) (2020) 2111.

[34] J. Ivorra-Martinez, M.A. Peydro, J. Gomez-Caturla, T. Boronat, R. Balart, The potential of an itaconic acid diester as environmentally friendly plasticizer for injection-molded polylactide parts, Macromol. Mater. Eng. 307 (12) (2022), 2200360.

[35] M. Maiza, A. Hamam, Toughened Poly (lactic acid)/Poly (ε-caprolactone) blend with triethyl citrate (TEC) and polyethylene glycol (PEG3), Polymer-Plastics Technology and Materials 61 (3) (2022) 276–282.

[36] M.P. Arrieta, J. López, E. Rayón, A. Jiménez, Disintegrability under composting conditions of plasticized PLA–PHB blends, Polym. Degrad. Stabil. 108 (2014) 307–318.

[37] I. Dominguez-Candela, J. Gomez-Caturla, S. Cardona, J. Lora-Garcia, V. Fombuena, Novel compatibilizers and plasticizers developed from epoxidized and maleinized chia oil in composites based on PLA and chia seed flour, Eur. Polym. J. 173 (2022), 111289.

[38] J. Ferri, D. Garcia-Garcia, L. Sánchez-Nacher, O. Fenollar, R. Balart, The effect of maleinized linseed oil (MLO) on mechanical performance of poly (lactic acid)-thermoplastic starch (PLA-TPS) blends, Carbohydr. Polym. 147 (2016) 60–68.

[39] R. Liu, Y. Peng, J. Cao, Y. Chen, Comparison on properties of lignocellulosic flour/polymer composites by using wood, cellulose, and lignin flours as fillers, Compos. Sci. Technol. 103 (2014) 1–7.
[40] A. Jordá-Vilaplana, V. Fombuena, D. García-García, M. Samper, L. Sánchez-Nácher, Surface modification of polylactic acid (PLA) by air atmospheric plasma treatment, Eur. Polym. J. 58 (2014) 23–33.
[41] Y. Zou, H. Zheng, X. Luo, J. Tang, Study on the influence of polar groups in pour point depressant on flow properties of Karamay crude oil, J. Dispersion Sci. Technol. (2023) 1–8.